

## RECONSTRUCTING JÖKULHLAUP DISCHARGE USING THE MORPHOLOGY OF ERODED VOLCANIC ROOTLESS CONES

KRYSTINA LINCOLN, Williams College  
Research Advisor: Bud Wobus

### ABSTRACT

Jökulhlaups are low frequency, high magnitude outburst flood events with incredible landscape altering potential given their catastrophic discharge, high velocities, and ability to mobilize sediment. The most recent in the Skaftá river originated from the Eastern Skaftá cauldron and reached peak flow on October 2<sup>nd</sup>, 2015. In this study, we used the high water marks recorded on rootless cones that lie within a braided segment of the river. Using high resolution aerial imagery and terrain models, mapped high water marks were used to construct an interpolated flood surface representing the peak flow. Preliminary discharge reconstructions along two cross sections of the flood area estimate the discharge at the site within one order of the true magnitude, with values ranging between 3200 m<sup>3</sup>/s and 8800 m<sup>3</sup>/s. These exceed the estimated peak discharge at the glacier margin (3000 m<sup>3</sup>/s) and the recorded discharge at an upstream gauging site (2100 m<sup>3</sup>/s). Discharge reconstruction is complicated by the non-uniform geometry of the field site, with numerous obstacles to flow. We suggest that the velocity (and thus discharge) is overestimated using Manning's equation, which does not account for the energy required to transport high suspended sediment concentrations. In the equations, the velocity accommodates all of the flow energy, but in reality, the energy driving the flow velocity would be less because some would be used to transport the sediment. Discharge reconstructions have an inherent amount of uncertainty, but high quality aerial imagery and terrain models, coupled with field observations, can successfully estimate peak flood discharge within an order of magnitude.

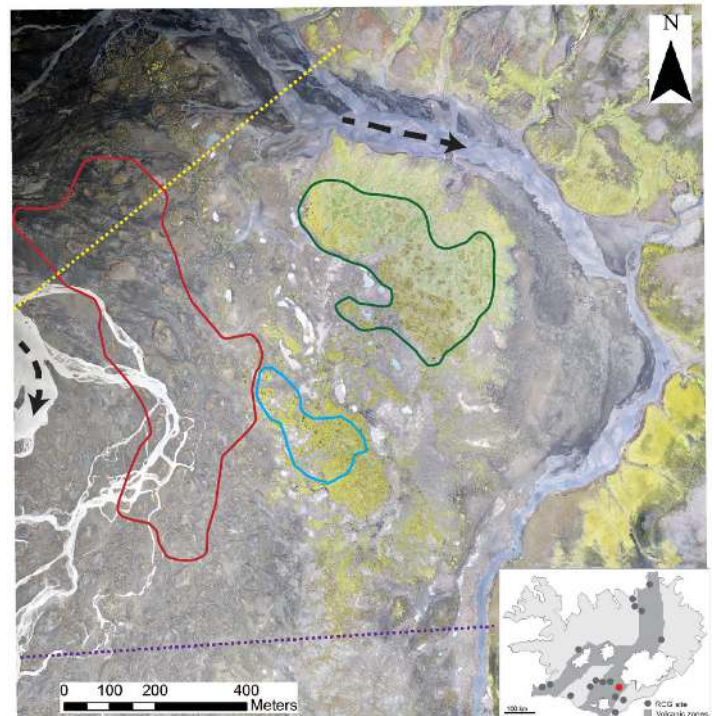


Figure 1. Orthoimage (4 cm/pixel) of the field site, showing water flow directions (dashed arrows) and the high (red), intermediate (blue) and pristine (green) zones of rootless cone erosion. The orthoimage extent is 1.6 km<sup>2</sup>. Yellow dotted line is the upstream transect for the discharge reconstruction, and the purple dotted line is the downstream transect. Inset map highlights approximate study area and other rootless cones groups in Iceland (modified from Fagents and Thordarson, 2007).

### INTRODUCTION

The Eastern Skaftá cauldron released a record-breaking outburst flood (jökulhlaup), with peak discharge on October 2<sup>nd</sup> 2015, inundating and eroding much of a rootless cone group (Fig. 1). The rootless cones were emplaced during the Laki fissure eruption of 1783–1784, young enough that the jökulhlaup

history of the river is fairly well constrained and there is a good estimate for how much erosion has impacted the cones.

We investigate how well major flood events can be reconstructed using high-resolution aerial imagery. High water marks and undercut sectors of the cones were each identified during ground-based examination, and we show they can be demarcated in aerial imagery. If accurate high water marks can be identified in the imagery, such a methodology could confidently be applied in studies of other major floods. Field observations can be used with stream gauging data and historic imagery to allow confident comparison of the existing erosion features with the recent event and smaller, semi-annual flood events in the Skaftá.

This investigation has implications for reconstructing paleo-hydrologic and paleo-environmental conditions in Iceland and on Mars. Given the strong evidence for catastrophic mega-floods in Iceland, constraining morphologic indicators at this site may allow for reconstruction of historic discharge rates elsewhere. Such information must be considered when planning major infrastructure projects like roads, bridges, and hydroelectric stations.

## JÖKULHLAUP HISTORY

Jökulhlaups occur when sub-glacial or englacial lakes drain to the glacial margin. Jökulhlaups are high magnitude, low frequency events, with tremendous landscaping potential because of their catastrophic discharge, sediment transport capacity, and sustained period of high flow (Magilligan et al., 2002; Björnsson, 2002, 2010; Old et al., 2005; Russell et al., 2006). Jökulhlaups in the Skaftá river originate from two geothermal fields, which create the Eastern and Western Skaftá cauldrons (Skaftákatlar), beneath the Vatnajökull ice sheet (Björnsson, 1977, 2002). More than 4,530 kg/s were transported in suspension during a moderate seven day Skaftá jökulhlaup in 1997 that had a discharge of 572 m<sup>3</sup>/s (Old et al., 2005). Sediment transport values are important for understanding the erosive capacity of the floods,

but they can be difficult to reconstruct because as jökulhlaups erode landforms, they simultaneously deposit and rework sediment.

Workers have closely studied jökulhlaups in the Skaftá since 1955 and historical personal accounts can trace smaller jökulhlaups in the Skaftá back to 1910 (Björnsson, 1977). These catastrophic events now occur almost yearly in the Skaftá. They are considered ‘fast-rising,’ reaching peak discharge within one to three days and waning over a period of two weeks (Björnsson, 1977, 2002). Flow measurements are recorded at the Sveinstindur gauging station, approximately 25 km downstream of the glacier margin and 8 km upstream of the rootless cone study site.

In late September/early October 2015, a jökulhlaup draining from the Eastern Skaftá cauldron released into the Skaftá River. Hydrologists first reported the flood beneath the glacier on September 29<sup>th</sup>, but floodwaters did not reach peak flow until October 2<sup>nd</sup>. This jökulhlaup had a peak discharge near 2,100 m<sup>3</sup>/s at the gauging site, making it the largest event in the Skaftá since the gauging site was established in 1971 and likely since at least 1955 when records began. Near the glacier margin, the discharge was estimated to be over 3,000 m<sup>3</sup>/s, approximately twice the discharge of the next largest jökulhlaup recorded in the Skaftá (Jóhannesson et al., 2016). The flood event caused a nearly fifteen-fold increase in discharge and a threefold increase in depth relative to the summer melt (Fig. 2).

The differences between the discharge estimate at the glacier margin and at the gauge are worth noting. It is possible that the flood at the gauging site exceeded the maximum depth that the site was equipped to measure, or it is equally as possible that the flood was not fully contained in the Skaftá channel between the margin and the gauging site. For our purposes, the former option would allow the best comparison between the estimate at the glacier margin and the geomorphically reconstructed discharge, but there is inherent uncertainty in this reconstruction.

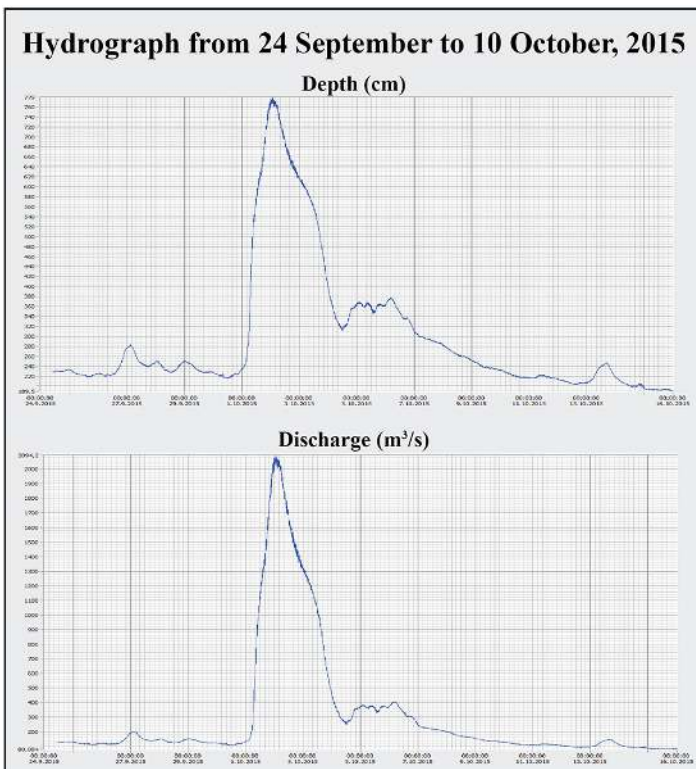


Figure 2. Discharge and water depth from the hydrograph at the Skaftá við Steinvensen gauging site, recording the jökulhlaup data from 24 September to 10 October, 2015. Note the peak flow near October 2<sup>nd</sup>.

## FIELD WORK

A two-person field team flew a Trimble UX5-HP fixed wing drone within a 1.6 km<sup>2</sup> flight box around the Úlfarsdalur rootless cone group, situated alongside and within the floodplain of the Skaftá river. The drone collected roughly 1400 geo-located images from a constant elevation of 120 m above the site.

During two days of the field campaign, a team worked to get a sense of cone group features, ground-truthing the aerially derived dataset. The team worked to photo-document and geo-locate type localities and to provide field descriptions of local features. Field photographs of high water marks were taken with a consistent scale, accompanied by sketches and a GPS position. When determining high water marks in the field, the field team looked for consistent heights along a cone where the surface was scoured, destabilized, or blanketed in river silt or sand. High water marks could be fairly well correlated from cone to cone (Fig. 3). In many areas, the field team noted that sectors of the cone failed after being destabilized in the high flow, producing a failure scarp which might be confused for



Figure 3. Well-matched high water marks (dashed yellow) between several rootless cones in the background of field photo. Photo by Andy de Wet, Franklin and Marshall College

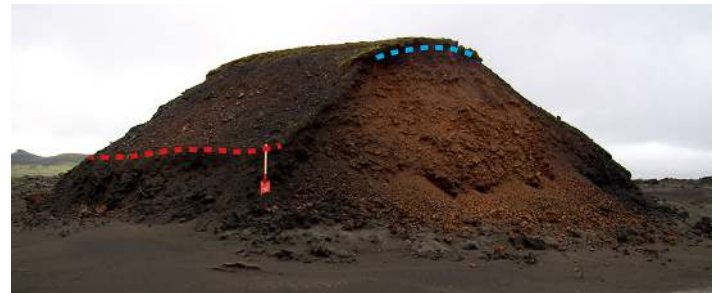


Figure 4. A rootless cone near waypoint 56, which has a high water mark (dashed red) and a failure scarp from flood induced undercutting and destabilization (dashed blue).

a high water mark in the remote sensing products (Fig. 4).

## REMOTE SENSING

### Imagery Processing

Drone imagery was processed using Trimble Business Center to create an ortho-rectified image with a ground resolution of 4 cm/pixel and a digital terrain model (DTM) with a ground resolution of 20 cm/pixel (Fig. 1). This process cannot accurately reconstruct moving surfaces, such as flowing rivers. A second iteration of the DTM was compiled at a lower resolution of 80 cm/pixel to reduce the amount of errors due to over interpolation in the water covered areas. The medium resolution DTM was edited using the ArcMap Raster Edit Suite (ARES) for ArcMap 10.3 add-on (Yu, 2015), which allows users to redefine individual pixels

or groups of pixels. Given the scope of the project, I only edited the DTM along the lines selected to construct cross-sections. Erroneous groups of pixels were easily identifiable, and their values were replaced using the median value of a neighboring group of non-erroneous pixels.

## Reconstructing the High Water Surface

Mapping the high water marks required close examination of field photographs, the aerial imagery, the DTM, a slope raster, and a curvature raster. The curvature raster represents the second derivative of the surface, which highlights breaks in slope. If the surface is upwardly convex at a given point, it is assigned a negative value (resulting in a black cell), but if the surface is upwardly concave, it is assigned a positive value (resulting in a white cell).

For example, the remote sensing products for the cone shown in Figure 4 are seen in Figure 5. In this instance, the slope steepens below the high water mark (dashed red line), which can be identified on the field photograph by the thin coating of river silts. On the slope raster, this could be identified as the transition between a medium grade, long, and regular slope, to a short, steep slope (red). Beneath the high water mark, the surface transitions from a planar surface, to one that is concave up, then convex up. Thus, when using the curvature raster to map this high water mark, the high water mark must be placed at the transition between the gray pixels and the white (positive) pixels. The elevation model is the least helpful mapping tool for this cone, but the elevation model does clearly show the failure scarp that followed destabilization from undercutting during the flood (dashed blue line in Figure 4).

Roughly 200 high water marks were mapped across the field area. I fit a trend interpolation to the mapped high water marks, modelling the surface of the water at peak flood depth, or at least the flood depth associated with velocities significant enough to do erosive work on the landscape. To evaluate the fit of the trend surface to the high water marks, I subtracted the interpolated trend surface from the elevation of the mapped high water to get the residuals at each mapped

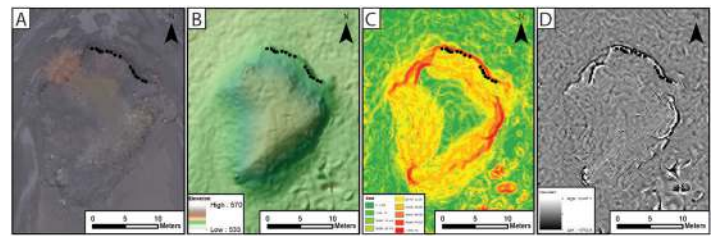


Figure 5. Remote sensing products used to assign high water mark points (red dots) along a rootless cone near waypoint 56. A) Orthorectified image. B) DTM draped over a hillshade. C) Slope raster. D) Curvature raster. In this instance, the field photograph (Fig. 4) showed that the slope greatly increased beneath the high water mark while the curvature transitioned from a fairly planar surface to a concave up surface, before transitioning to a convex up surface with the blanket of river silts. High water marks needed to be placed above the transition to a steeper slope and the concave up surface.

point. I removed three outliers from the mapped high water points, and ran the interpolation and residual calculating process again. When run without the outliers, the residuals are normally distributed, ranging from 0.857 m to 1.089 m, with a mean of 0.000 m and standard deviation of 0.406 m.

## Calculating Flood Discharge

Four transect lines were selected across the field area for discharge reconstruction and the results of two are reported here. During the flood, flow direction deviated from the normal flow paths, so the transect lines were established perpendicular to the apparent flood pathway evidenced by the erosive deposits. Preliminary work has characterized the flood depths, velocity and discharge of two transects, using the panel method to apply Manning's equation ( $V = D^{2/3} * S^{1/2} / n$ ) and the discharge equation ( $Q = W * D * V$ ). In these calculations, V is velocity (m/s), D is depth (m), S is slope (m/m), W is width (m), and Q is discharge ( $m^3/s$ ). At this site, the calculations were completed using slopes of 0.0015 m/m and 0.002 m/m, and 0.035 and 0.045 for Manning's constant. Einarsson (2009) suggested an n value of 0.035 for the Skaftá riverbed, but we used a range of higher values because of the rootless cones and vegetated terrain in this braided section of the river. The terrain model did not encapsulate the full flow pathway, so the areas outside the boundaries were assigned the depth of the closest panel.

## RESULTS

For the 870 m upstream profile (yellow dotted line in Figure 1), the panel depths varied between 1.4 m and 3.3 m, resulting in velocities between 1.1 m/s and 2.8 m/s. When calculated with a slope of 0.0015 and a Manning's  $n$  value of 0.035, the total discharge was 4120 m<sup>3</sup>/s. In varying the slopes and  $n$  values, I calculated discharges ranging from 3200 m<sup>3</sup>/s to 4750 m<sup>3</sup>/s.

At the 1050 m long downstream profile (purple dotted line in Figure 1), panel depths ranged between 1.3 m and 3.2 m. This led to similar velocities as the upstream profile, varying between 1.1 m/s and 2.8 m/s. With a reasonable slope of 0.0015 m/m and a Manning  $n$  value of 0.035, the total discharge was 7610 m<sup>3</sup>/s. When the slopes and  $n$  values were varied, the range of discharges spanned from 6660 m<sup>3</sup>/s to 8790 m<sup>3</sup>/s.

## DISCUSSION

Preliminary results suggest that this method overestimates jökulhlaup discharge at this site, when compared to the estimated discharge at the glacier margin (3000 m<sup>3</sup>/s) and the recorded discharge at the gauging site 28 km upstream (2100 m<sup>3</sup>/s). Our calculations are complicated by the inconsistent shape of the channel, especially because the water reaches the site directly after being channeled through a waterfall just northwest of the imagery. While the residuals of the interpolated high water surface were reasonable, the surface accuracy may have been limited due to the lack of any mapped high water marks in the most southern 300 meters of the imagery. Field evidence in this region suggested that the area was underwater, but the area does not preserve high water marks. It should be expected that the flow would thin and slow as it spread out in that region, after navigating the congested rootless cone area.

It may also be likely that some of the mapped high water marks were recorded as such because the flow was locally obstructed. This could lead to an overestimation of the reconstructed high water surface across the field site, and explain the overestimation of discharge. If we were to assume that the interpolated high water surface is accurate, it is difficult to assign a representative Manning's  $n$  value for the field site.

Trenches dug in the field suggest that the flood may have deposited or mobilized over a meter of sediment in the area of the eroded rootless cones, making it hard to understand exactly what substrate the flow encountered across the field site. Currently the area is blanketed in river sands, but at the base of the rootless cones would be lava crusts.

The largest factor causing uncertainty in our calculations is likely the high suspended sediment concentration in the flood waters, which may become even more highly concentrated as the flow encounters the rootless cone group. It is clear that the rootless cones were highly scoured in the event, and a proportion of the flood energy would have to contribute to the transport of the sediment at the expense of higher velocity. Manning's equation assumes that the water is clear and no energy is required to sustain sediment transport, and this assumption is violated in the case of jökulhlaups, especially one that travels through a rootless cone field. Rootless cones are made of fairly loose, fragmented lava spatter clasts and minor agglutinated layers, and much of this material was mobilized in the flood event. Our reconstruction does not consider the energy that would be needed to transport the sediments, resulting in overestimates of the velocity and discharge. This consideration is especially important for the most downstream profile. Velocities there may have been overestimated because the flow picked up additional sediment as it passed through the rootless cone group.

## CONCLUSIONS

When used in tandem with ground-truthed high water marks and field photos, high resolution aerial imagery and terrain models can be successfully used to reconstruct peak flood discharge within an order of magnitude. Peak discharge surfaces can be interpolated from mapped points with reasonable accuracy when using a high resolution terrain model, as high water marks can be clearly located using curvature and slope rasters. Further work understanding the relationship between suspended sediment concentration and its impact on flow velocities would increase the accuracy of this reconstruction, as velocities and discharges were likely overestimated because the calculations neglected the

energy that would sustain the sediment transport.

## ACKNOWLEDGEMENTS

I would like to thank my Keck group for laughs in the field; Andy deWet, Christopher Hamilton, and Stephen Scheidt for handling logistics, managing data, and helping to develop my project; Anny Sainvil for putting up with my antics across the globe; and Bud Wobus, David Dethier, and Cory Campbell for supporting my project back at Williams. This work was supported by the Keck Geology Consortium, The National Science Foundation (grant number NSF-REU 1358987), and ExxonMobil Corporation.

## REFERENCES

- Björnsson, H., 1977, The Cause of Jökulhlaups in the Skafta River, Vatnajökull: *Jökull*, v. 27, p. 71–78.
- Björnsson, H., 2002, Subglacial lakes and jökulhlaups in Iceland: *Global and Planetary Change*, v. 35, p. 255–271.
- Björnsson, H., 2010, Jökulhlaups in Iceland: Sources, Release and Drainage: Iceland in the Central Northern Atlantic: hotspot, sea currents and climate change, p. 1–14.
- Einarsson, B., 2009, Jökulhlaups in Skaftá: A study of a jökulhlaup from the Western Skaftá cauldron in the Vatnajökull ice cap, Iceland [Ph.D. thesis]: University of Iceland, 90 p.
- Fagents, S.A., and Thordarson, T., 2007, Rootless volcanic cones in Iceland and on Mars, in Chapman, M., ed., *The Geology of Mars: Evidence from Earth-Based Analogs*: chap. 6, Cambridge, Cambridge University Press, p. 151–177.
- Greeley, R., and Fagents, S.A., 2001, Icelandic pseudocraters as analogs to some volcanic cones on Mars: *Journal of Geophysical Research*, v. 106, no. E9, p. 20,527–20,546.
- Jóhannesson, T., 2002, The initiation of the 1996 jökulhlaup from Lake Grímsvötn, Vatnajökull, Iceland: *The Extremes of the Extremes: Extraordinary Floods*, v. 271, no. 271, p. 57–64.
- Magilligan, F.J., Gomez, B., Mertes, L.A.K., Smith, L.C., Smith, N.D., Finnegan, D., and Garvin, J.B., 2002, Geomorphic effectiveness, sandur development, and the pattern of landscape response during jökulhlaups: Skeiðarársandur, southeastern Iceland: *Geomorphology*, v. 44, p. 95–113.
- Old, G.H., Lawler, D.M., and Snorrason, Á., 2005, Discharge and suspended sediment dynamics during two jökulhlaups in the Skaftá river, Iceland: *Earth Surface Processes and Landforms*, v. 30, no. 11, p. 1441–1460.
- Russell, A.J., Roberts, M.J., Fay, H., Marren, P.M., Cassidy, N.J., Tweed, F.S., and Harris, T., 2006, Icelandic jökulhlaup impacts: Implications for ice-sheet hydrology, sediment transfer and geomorphology: *Geomorphology*, v. 75, p. 33–64.
- White, O.L., 2010, *The Influence of Environmental Conditions on volcanic processes on the terrestrial planets* [Ph.D. thesis]: University College London, 291 p.
- Yu, H., Wang, X., Qing, J., and Nie, H., ArcMap Raster Edit Suits (ARES) version 0.2.1 (for ArcMap 10.3), 2015, GitHub repository, <https://github.com/haoliangyu/ares>.